Neurobiology of Aging 36 (2015) 2885–2892

Contents lists available at ScienceDirect

Neurobiology of Aging

journal homepage: www.elsevier.com/locate/neuaging

Therapeutic potentials of human adipose-derived stem cells on the mouse model of Parkinson's disease

Hee Soon Choi [a,1], Hee Jin Kim [b,1], Jin-Hwan Oh [c], Hyeong-Geun Park [d], Jeong Chan Ra [d], Keun-A. Chang [c,e,**], Yoo-Hun Suh [e,f,g,*]

[a] Research Division, Department of Structure and Function of Neural Network, Korea Brain Research Institute, Daegu, Korea
[b] Research Division, Department of Neural Development and Disease, Korea Brain Research Institute, Daegu, Korea
[c] Neuroscience Research Institute, Gachon University, Incheon, Korea
[d] K-STEM CELL Institute, Seoul, Korea
[e] Department of Pharmacology, Gachon University, Incheon, Korea
[f] Korea Brain Research Institute, Daegu, Korea
[g] Department of Pharmacology, Seoul National University Medical College, Seoul, Korea

ARTICLE INFO

Article history:
Received 23 January 2015
Received in revised form 15 June 2015
Accepted 15 June 2015
Available online 24 June 2015

Keywords:
Human adipose-derived stem cells
6-OHDA
Parkinson's disease
Mitochondria

ABSTRACT

The treatment of Parkinson's disease (PD) using stem cells has long been the focus of many researchers, but the ideal therapeutic strategy has not yet been developed. The consistency and high reliability of the experimental results confirmed by animal models are considered to be a critical factor in the stability of stem cell transplantation for PD. Therefore, the aim of this study was to investigate the preventive and therapeutic potential of human adipose-derived stem cells (hASC) for PD and was to identify the related factors to this therapeutic effect. The hASC were intravenously injected into the tail vein of a PD mouse model induced by 6-hydroxydopamine. Consequently, the behavioral performances were significantly improved at 3 weeks after the injection of hASC. Additionally, dopaminergic neurons were rescued, the number of structure-modified mitochondria was decreased, and mitochondrial complex I activity was restored in the brains of the hASC-injected PD mouse model. Overall, this study underscores that intravenously transplanted hASC may have therapeutic potential for PD by recovering mitochondrial functions.

1. Introduction

Parkinson's disease (PD) is the second most common neurodegenerative disease. The onset rate is estimated to be about 1%–2% of individuals aged >60 years and >3% of the number aged >75 years (Gasser, 2009; Pankratz and Foroud, 2007). Aging, genetic and environmental factors are jointly involved in the development of PD, though the exact mechanism was poorly understood. Especially, many epidemiological studies have reported that aging is the greatest risk factor for PD (Bennett et al., 1996; Morens et al., 1996; Tanner and Goldman, 1996). The signs and symptoms of PD are slow movement, rigidity, and tremor because of the loss of dopaminergic neurons in the substantia nigra (SN) that project to the striatum (Murrell et al., 2008). The progressive degeneration and loss of dopaminergic neurons in the SN are accompanied by the formation of intraneuronal inclusions, called "Lewy body," that are primarily composed of α-synuclein (Spillantini et al., 1997). However, no treatment has yet been developed because their interplay is still unclear. Lately, PD treatments have tried to compensate for the loss of striatal dopamine by administering its precursor L-DOPA and/or dopamine D2 receptor agonists (Collier et al., 2011; Dragicevic et al., 2014; Gazewood et al., 2013; Olanow and Schapira, 2013).

Recently, stem cell therapy for PD has been in the spotlight. The ideal transplantable cell should be easily accessible, have a high proliferation capacity in vitro, and have the ability to undergo differentiation into multiple cell lineages such as astrocytes, oligodendrocytes, and neuronal cells. In recent studies, human adipose-derived stem cell (hASC), a type of mesenchymal stem cell (MSC) isolated from adipose tissue, are well known for their pluripotent ability to differentiate into neuron-like cells

* Corresponding author at: Korea Brain Research Institute (KBRI), Daegu, 701-300, South Korea, Tel.: +82-53-980-8101; fax: +82-53-980-8239.
** Corresponding author at: Department of Pharmacology, Gachon University, Incheon, 406-799, South Korea, Tel.: +82-32-820-4332, fax: +82-32-820-4744
E-mail addresses: keuna705@gachon.ac.kr (K.-A. Chang), yhsuh@snu.ac.kr (Y.-H. Suh).
[1] Hee Soon Choi and Hee Jin Kim equally contributed to this work.

http://dx.doi.org/10.1016/j.neurobiolaging.2015.06.022

(Chang et al., 2014; Kim et al., 2012). Autologous hASC has significant advantages, such as the lack of immune rejection responses, tumorigenesis, and ethical problems (Tomita et al., 2013; Zuk et al., 2002). Moreover, ASCs have already been used for some clinical applications (Traktuev et al., 2008). Unlike stem cells derived from other sources and induced pluripotent stem cells (Amariglio et al., 2009; Bjorklund et al., 2002; Brederlau et al., 2006; Duinsbergen et al., 2009), MSCs show a low probability of being tumorigenic, and a recent phase I study demonstrated the safety of MSC transplantation into PD patients (Glavaski-Joksimovic and Bohn, 2013; Venkataramana et al., 2010). Additionally, in our previous study, we found using an in vivo imaging technique that intravenously transplanted hASC could pass through the blood-brain barrier and migrate into the injuries of the brain (Chang et al., 2014; Kim et al., 2012). For these reasons, hASC may be the optimal stem cells for clinical therapies.

In many studies, it has been previously described that the structural and functional alterations of mitochondria were associated with neurodegenerative diseases including PD. The genes related to PD, such as α-synuclein, parkin, DJ-1, and PINK1, are directly or indirectly involved with mitochondrial functions (Shim et al., 2011). Mitochondria supply adenosine triphosphate to the cell through oxidative phosphorylation, synthesize key molecules, and buffer calcium gradients (Frazier et al., 2006). Therefore, mitochondrial health is closely associated with the metabolic component. Aging and energy-dependent disturbances involve mitochondrial defects (Wang et al., 2013b). In particular, impaired function of mitochondria leads to increased oxidative stress or reactive oxygen species, and both have a significant pathogenic role in the selective loss of dopaminergic neurons in human patients and in PD mouse models (Dexter et al., 1989; Moon et al., 2013; Sriram et al., 1997).

Traditionally, the experimental models for PD have been created in rodents and primates via the delivery of neurotoxins, such as 6-hydroxydopamine (6-OHDA) (Stott and Barker, 2014). It has been reported that 6-OHDA is a dopamine analog that specifically induces dopaminergic neuronal cell death via either uncoupling mitochondrial oxidative phosphorylation, resulting in energy deprivation or alternatively through its ability to produce hydrogen peroxide, hydroxyl, and superoxide radicals (Soto-Otero et al., 2008; Wang et al., 2013b). 6-OHDA is also known to inhibit complexes I and IV of the mitochondrial respiratory chain in the SN (Ben-Shachar et al., 1995; Glinka and Youdim, 1995; Glinka et al., 1996; Mizuno et al., 1989).

In the present study, we focused on the applicability of hASC by a convenient and safe intravenous injection and the relevance of hASC to mitochondrial functions in a PD mouse model induced by 6-OHDA for the first time. We investigated whether hASC injection could rescue the behavioral deficits in the PD mouse model using the apomorphine-induced rotation test and the rotarod performance test. To confirm a neuropathological difference, we evaluated the change in the numbers of tyrosine hydroxylase (TH)-positive neurons in hASC-injected PD mice compared with sham control PD mice. To assess whether injected hASC rescued alterations in the dopamine level in the striatum, we performed positron emission tomography (PET) imaging analysis with [^{11}C]raclopride, an antagonist of DA-D2R, in the PD mouse model injected with hASC or saline. Additionally, we focused on changes in the mitochondrial structure and complex I activity in the experimental PD model.

2. Experimental procedures

2.1. Materials

hASCs (RNL-Bio_SM081201 P3), male C57BL6 mice, desipramine, apomorphine, 6-OHDA (Sigma Aldrich Korea, Kyounggi-do, Korea), 25% glutaraldehyde (Electron Microscopy Sciences, PA, USA), Dako EnVision+ system–horseradish peroxidase–labeled polymer (Dako Korea, Seoul, Korea), DAB+ substrate chromogen (Dako Korea), anti-TH antibody (Santa Cruz Biotechnology, CA, USA), and the complex I enzyme activity microplate assay kit (Abcam, Cambridge, UK) were used in the experiments.

2.2. Method

2.2.1. PD mouse model preparation and behavioral testing

Seven-week-old male C57BL/6N mice weighing 20–25 g were housed in a specific pathogen-free room, automatically maintained on a 12-hour light-dark cycle at 25 °C and proper humidity, and were given food and water ad libitum. Desipramine (25 mg/kg, Sigma, St. Louis, MO, USA) was injected intraperitoneally (ip) to block norepinephrine reuptake 1 hour before 6-OHDA injection. The animals were anesthetized with Rompun and Zoletil (1 μg/g, ip) and injected with 10 μg of 6-OHDA (4 μg/μL containing 0.2 mg/mL L-ascorbic acid) or the same volume of saline for the PD model or control, respectively. 6-OHDA or saline was injected unilaterally into the SN (A/P = −3.2, M/L = −1.5, D/V = −4.6) with a flat skull position (coordinates in mm, with anterior-posterior and lateral coordinates measured from bregma, and ventral from dura) using a Kopf stereotaxic frame (Kopf Instruments, Tujunga, CA, USA). The injections were made at a rate of 0.5 μL/min using a 25-gauge Hamilton syringe (Hamilton Company, NV, USA). The in vivo experimental protocol that followed is shown in Fig. 1A. After the surgery, each mouse was kept in an individual cage.

Two weeks after the 6-OHDA injection, motor coordination, and fatigue resistance were tested using the accelerating rotarod and apomorphine-induced rotation tests for the measurement of baseline behavior (n = 10 per group). The control mouse and PD mouse induced by saline or 6-OHDA, respectively, was selected by the baseline behavior testing and distributed to each group. The injection of hASC (1×10^6 cells) was conducted twice at an interval of 2 weeks, and the behavioral performances were measured at 3 weeks after the final injection of hASC via the rotation and accelerating rotarod tests. For the rotation test, mice were habituated in the basket for 10 minutes. After subcutaneous injection with apomorphine (0.05 mg/kg), the behavior of the mouse was tracked and the number of right and left rotations and the net number of rotations for 30 minutes were analyzed by an EthoVision video tracking system. For the rotarod test, mice were conditioned at a speed of 8 rpm for 5 minutes and at a speed of 12 rpm for 5 minutes at an interval of 1 hour. One day after the training, the motor performance was tested at an accelerated speed from 2 rpm to 20 rpm for 10 minutes. The time schedule of the experimental procedure is shown in Fig. 1.

2.2.2. Micro-positron emission tomography

The PET study with [^{11}C]raclopride was performed 4–5 weeks after the 2nd adipose-derived stem cells treatment (n = 4 per group). Anesthesia was induced and maintained with passive 1.5% isoflurane at an oxygen level of 1.5 L/min with vacuum. Each mouse was positioned on a bed with its brain centered in the gantry. The PET scan was performed using a Focus 120 Micro PET system (Concorde Microsystems, Knoxville, USA). Dynamic scans were performed for 90 minutes immediately after a [^{11}C]raclopride injection (18.50–24.64 MBq, 200 μL) via the tail vein. The acquisition of data was reconstructed with a 2D-filtered back-projection algorithm (microPET Manager, Siemens Medical Solutions, Knoxville, USA). The dynamic frame was composed of 32 frames: 1 × 60 seconds, 6 × 20 seconds, 2 × 30 seconds, 5 ×

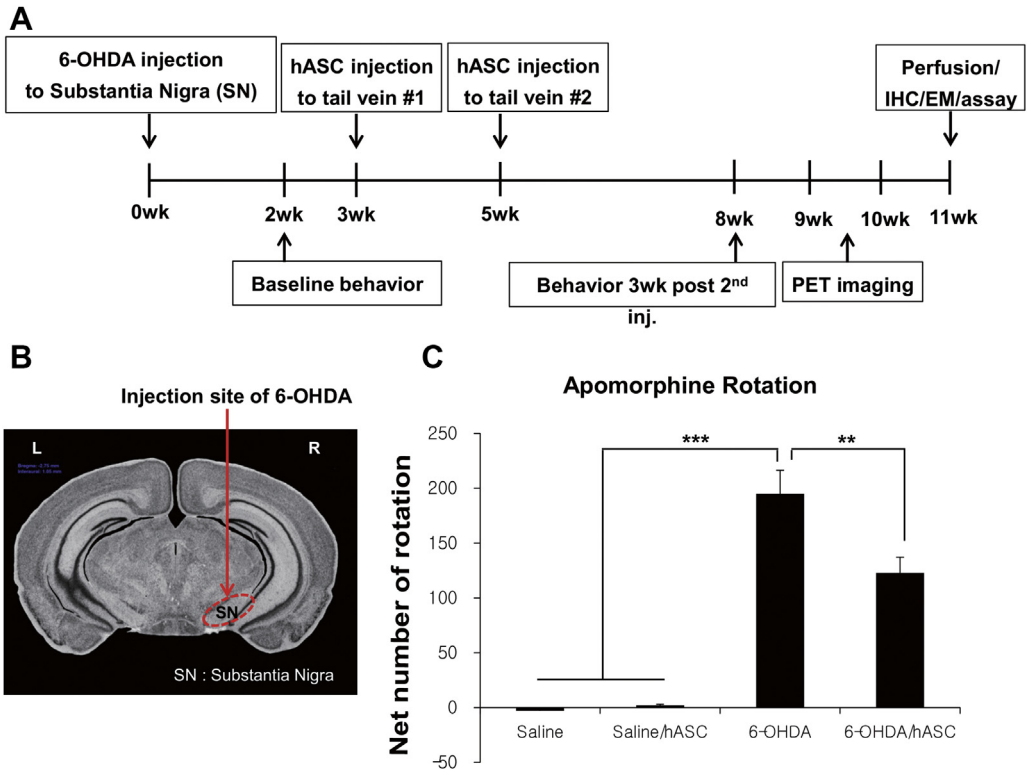

Fig. 1. The motor performances were improved in hASC-transplanted PD mice. (A) 6-OHDA was injected into the SN of 6-week-old male mice and the baseline behavior tests were performed at 2 weeks after the drug injection for the selection of the PD mouse model. hASC were transplanted twice at 3 weeks and 5 weeks after the 6-OHDA injection. Behavioral assessments via the rotarod and rotation tests were performed at 3 weeks after the second injection of hASC. positron emission tomography images were obtained at 5 weeks after the second injection of hASC, and the mice were sacrificed next week. (B) The 6-OHDA was stereotaxically injected into the SN (AP, −3.2 mm; ML, −1.5 mm; DV, −4.6 mm). (C) The number of rotation induced by apomorphine was increased in PD mice and significantly decreased in the hASC-injected group. (Average number of rotation, saline, −3 ± 1; saline and/or hASC, 2 ± 1; 6-OHDA, 195 ± 21; 6-OHDA and/or hASC, 123 ± 14) ***$p < 0.001$; **$p < 0.01$ by 1-way analysis of variance, Tukey's multiple comparisons test. Abbreviations: hASC, human adipose-derived stem cells; IHC, immunohistochemistry; 6-OHDA, 6-hydroxydopamine; PET, positron emission tomography.

60 seconds, 2 × 120 seconds, 4 × 240 seconds, 12 × 300 seconds. For the quantitative analysis, the reconstructed PET images were analyzed with PMOD software (PMOD Technologies Ltd, Zurich, Switzerland). The region of interest was set up as the left and right striatum. The binding potential was measured in each region of interest.

2.2.3. Immunohistochemistry

The mice were anesthetized with Rompun and Zoletil (1 μg/g, ip) and transcardially perfused by saline with heparin after the completion of the behavioral tests. All the hemispheres were fixed overnight in 4% paraformaldehyde at 4 °C and embedded with paraffin. Coronal sections (4 μm) of paraffin-embedded hemispheres were cut through the entire SN using a microtome (Thermo Electron Corporation, OH, USA).

The brain slides were placed in a 55 °C oven for 10 minutes to melt the paraffin, rinsed in xylene for deparaffinization, and dehydrated using a descending ethanol series. The sections were retrieved by 0.01-M citric acid (pH 6.0) for 10 minutes at 60 °C and blocked with 0.5% triton X-100% and 2% normal serum in Tris-buffered saline. The sections were incubated in primary antibody (TH; 1:100) overnight at 4 °C and were incubated with Dako EnVision+ system–horseradish peroxidase–labeled polymer for 30 minutes. After washing in Tris-buffered saline, the tissue slides were incubated with liquid DAB+ substrate chromogen (Dako) for 10–30 minutes at room temperature. The sections were rinsed gently with distilled water and coverslipped with histomount (Invitrogen) (Kim et al., 2014). Each experiment was repeated 3 times (n = 3 per group).

2.2.4. Transmission electron microscopy

For the transmission electron microscope (TEM) observations, the mouse brains were isolated and fixed with 2.5 % glutaraldehyde in 0.1-M phosphate buffer (pH 7.4). The SN region was isolated, sufficiently fixed and cut into 1 × 1 × 1 mm cubes; a fixation solution was used to prevent the tissue from drying. Then, the tissue cubes were washed in cacodylate buffer, postfixed with 1% osmium tetroxide–phosphate-buffered saline (PBS) solution for 1 hour, dehydrated in a graded series of ethanol, infiltrated with propylene oxide, and embedded in Epon (Xu et al., 2012). Ultrathin sections were prepared and counterstained with 4% uranyl acetate and lead citrate (Shirpoor et al., 2009). TEM images were then obtained using a JEOL TEM (JEM-1400; Seoul National University Hospital Medical Research Institute, Seoul, Korea) at an accelerating voltage of 80 keV (Oh et al., 2010). The numbers of total and damaged mitochondria were counted in 2–5 frames per cell in the 5 cells for each brain sample (n = 3 per group).

2.2.5. Mitochondrial complex I activity assay

The brain samples were homogenized with PBS containing a protease inhibitor cocktail. The proteins were extracted by adding detergent and centrifuging at 12,000*g* for 20 minutes. All samples were diluted to a suitable concentration in the incubation solution. The prepared samples were added into the microplate and incubated for 3 hours at room temperature. Afterward, the wells were emptied by turning the plate over and rinsed twice with buffer. The assay solution was added into the emptied wells and any bubbles were removed as rapidly as possible. The plate was placed in the reader, and kinetic measurements were recorded at 450 nm

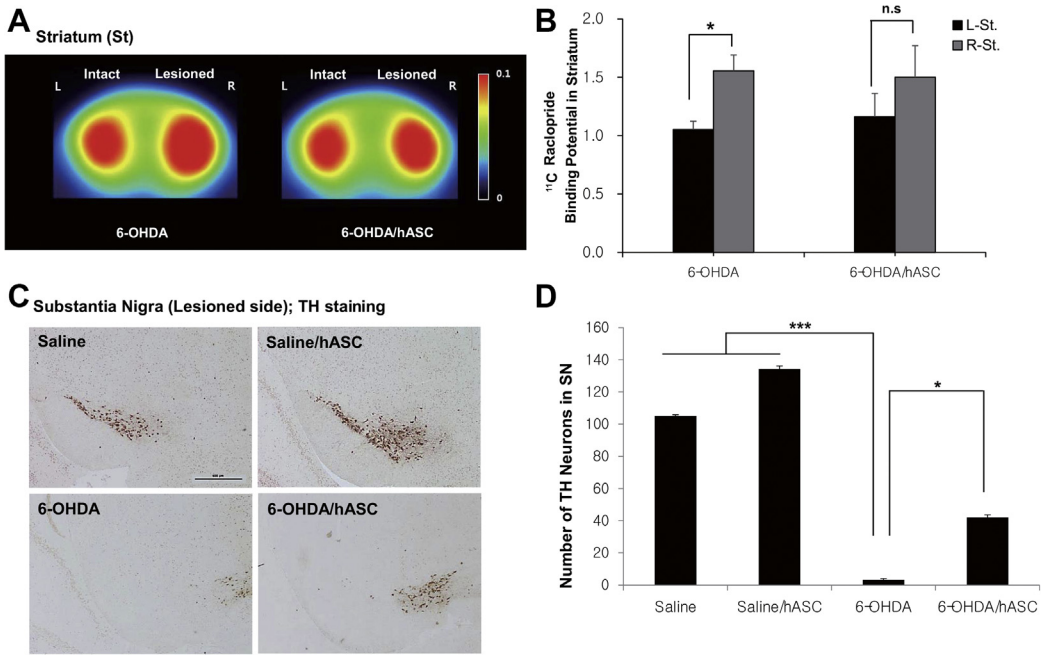

Fig. 2. The striatal dopamine transmission was restored and loss of dopaminergic neurons was decreased by the transplantation of hASC. The binding of dopamine with dopamine D2 receptors was measured in the striatum by the representative summed positron emission tomography (PET) images at 5 weeks after the second injection of hASC. (A) The images of the striatum of the 6-OHDA- or 6-OHDA and/or ASC-injected mouse were acquired by PET using [^{11}C]raclopride. The binding of [^{11}C]raclopride to dopamine D2 receptors was decreased in the hASC-injected PD mouse model compared to the PD mouse (left; normal, right; lesion). (B) A numerical value of binding potential is shown in a graph. The graph indicates the difference of value between the normal side and the lesioned side of the 6-OHDA- or 6-OHDA and/or ASC-injected mouse. There was no significant difference in the hASC-injected PD mouse. (C) The brain slices were immunostained with an anti-TH antibody. TH-positive dopaminergic neurons were visualized by DAB staining for light microscope observation. Dopaminergic neuronal cell death in the SN was sharply increased after the injection of 6-OHDA, and the dopaminergic neurons recovered with the hASC transplantation. (D) Dopaminergic neurons were counted and are shown by a graph. (Average number of TH-positive cells, saline, 105 ± 0.86; saline and/or hASC, 134 ± 1.84; 6-OHDA, 3.33 ± 0.62; 6-OHDA and/or hASC, 42 ± 1.69) $^{***}p < 0.001$; $^{*}p < 0.05$ by 1-way analysis of variance, Fisher's lysergic acid diethylamide test. Abbreviations: hASC, human adipose-derived stem cells; 6-OHDA, 6-hydroxydopamine; SN, substantia nigra; TH, tyrosine hydroxylase.

for 30 minutes at an interval of 1 minute. Each experiment was repeated 3 times (n = 3 per group).

2.3. Ethics statement

The animals used in this experiment were handled in accordance with the Guidelines for Animal Experimentation. This study was approved by the Ethics Committee of Seoul National University Institutional Animal Care and Use (SNU IACUC; approval ID; SNU100819-1–2).

2.4. Statistical analysis

The relationship among the groups was determined by Student *t* test and 1-way analysis of variance using GraphPad Prism 6 (GraphPad software, CA, USA). *p*-Values < 0.05 were considered statistically significant ($^{*}p < 0.05$; $^{**}p < 0.01$; $^{***}p < 0.001$).

3. Results

3.1. Intravenously transplanted hASC improved motor performances in the 6-OHDA-induced PD mouse model

To determine the effects of hASC transplantation in PD, hASC was intravenously transplanted into the tail-vein of the sham control or 6-OHDA-induced PD mice. Because 6-OHDA, as a specific catecholaminergic neurotoxin, is not able to cross the blood-brain barrier, stereotaxical injection of 6-OHDA into the SN is necessary to cause the nigrostriatal damage.

Next, the functional impairments were monitored by rating animal rotations induced by apomorphine and evaluating maximal motor performance using the accelerating rotarod test (Fig. 1). Because our PD mouse model had unilateral nigrostriatal damage in the right hemisphere, the rotational behavior by apomorphine, a dopamine receptor agonist, was used to investigate nigrostriatal function. 6-OHDA-injected mice spontaneously exhibited severe full-body contralateral rotations after a single subcutaneous administration of apomorphine (Fig. 1C). In contrast, the hASC-injected PD mice showed significantly decreased net rotations (average number of rotation, saline, −3 ± 1; saline and/or hASC, 2 ± 1; 6-OHDA, 195 ± 21; 6-OHDA/hASC, 123 ± 14).

The accelerating rotarod result showed that the motor coordination and fatigue resistance were improved in the hASC-injected PD group compared with the PD group (Supplementary Fig. 1). No difference was observed between the saline-injected and saline and/or hASC-injected groups (Supplementary Fig. 1). PD mice dropped quickly from the rotarod with less movement, but the hASC-injected PD mice endured for more time and had better movement on the rotarod than the PD mice (Supplementary Fig. 1) (Average time, saline, 481 ± 23; saline and/or hASC, 511 ± 22; 6-OHDA, 201 ± 14 seconds; 6-OHDA and/or hASC, 257 ± 25 seconds). Behavioral tests were performed at 3 weeks after the intravenous injection of hASC or saline and were measured by the apomorphine rotation and accelerating rotarod tests.

Our data clearly show that the intravenously engrafted hASC alleviated some of the motor system dysfunction.

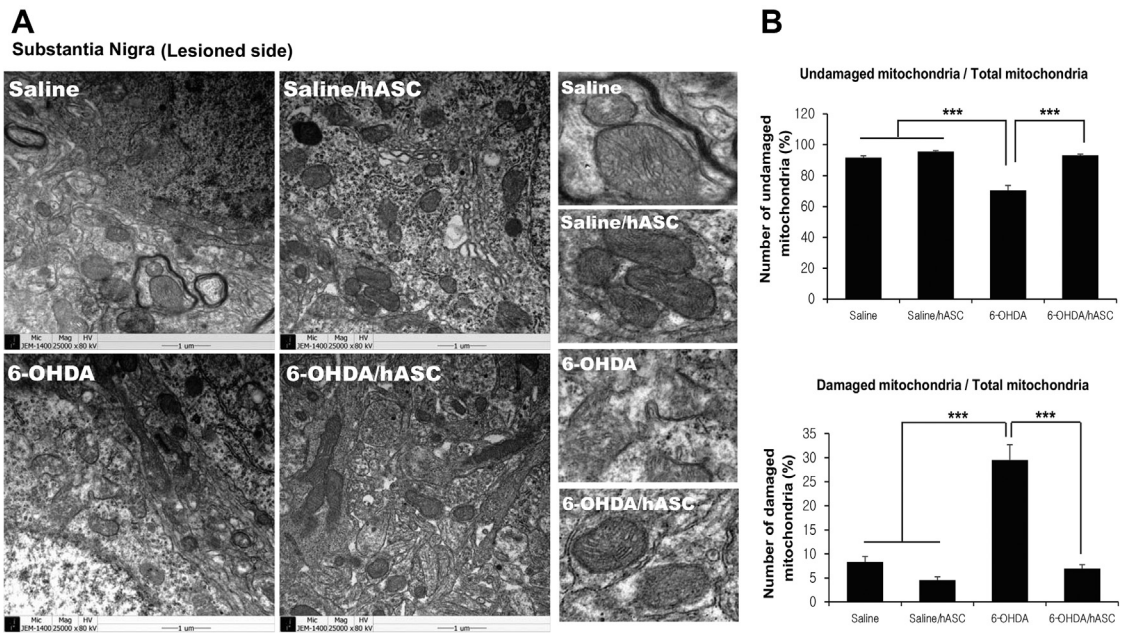

Fig. 3. Damaged mitochondria were rescued by the transplantation of hASC in PD mice. Mitochondrial images were obtained by transmission electron microscope. (A) Damaged and undamaged mitochondria were counted on the 15 fields of 5 cells in the substantia nigra isolated from each brain sample. The ruptured and impaired mitochondria were increased in 6-OHDA-injected mice and decreased by hASC injection. The enlarged images of the areas marked with an asterisk are indicated on the right. (B) The percentage of normal or damaged mitochondria is represented by a graph. (Normal mitochondria, saline, 91.66 ± 1.13; saline and/or hASC, 95.46 ± 0.71; 6-OHDA, 70.50 ± 3.18%; 6-OHDA and/or hASC, 93.06 ± 0.85%) ***$p < 0.001$ by 1-way analysis of variance, Tukey's multiple comparisons test. Abbreviations: hASC, human adipose-derived stem cells; 6-OHDA, 6-hydroxydopamine.

3.2. Intravenously transplanted hASC rescued dopaminergic neuronal cell death in the 6-OHDA-induced PD mouse model

To assess dopaminergic neuropathology, a PET imaging analysis was performed in 6-OHDA-injected or 6-OHDA and/or hASC-injected mice using raclopride (*S*-(−)-3,5-dichloro-*N*-[(ethyl-2-pyrrolidinyl)]methyl-2-hydroxy-6-methoxybenzamide) as a PET tracer. Raclopride, a dopamine D_2 receptor antagonist, was radiolabeled with ^{11}C ([^{11}C]raclopride) for imaging dopamine D_2 receptors in the striatum and to assess the degree of dopamine binding. The destruction of dopaminergic neurons in the SN by 6-OHDA leads to the consecutive depletion of dopamine in the striatum. Consequently, PD mice showed a marked increase in [^{11}C] raclopride binding to dopamine D2 receptors (Fig. 2A, left). In contrast, hASC-injected PD mice showed decreased binding of [^{11}C] raclopride with the dopamine D2 receptor according to the recovery of dopamine in the striatum (Fig. 2A, right). A numerical value of binding potential is shown in Fig. 2B. Striatal [^{11}C]raclopride binding potential in the PD mouse was significantly different between the left striatum (1.05 ± 0.06) and right striatum (1.56 ± 0.14). In contrast, the binding potential in the hASC-injected PD mouse exhibited no significant difference between the left striatum (1.16 ± 0.20) and right striatum (1.50 ± 0.27). This result indicates that the transplantation of hASC decreased difference in the binding between the left striatum (intact) and right striatum (lesioned) value.

We also examined the neuroprotective effect of hASC transplantation on 6-OHDA-induced dopaminergic neuronal cell death. Brain sections from each group were prepared from a paraffin block and immunostained with an anti-TH antibody. TH-positive dopaminergic neurons were severely decreased by the injection of 6-OHDA and significantly recovered with hASC transplantation (Fig. 2C). When the number of TH-positive dopaminergic neurons in the SN for each group was counted and quantified, a significant difference was found between the 6-OHDA and 6-OHDA and hASC group (Average number of TH positive cells, saline, 105 ± 0.86; saline and/or hASC, 134 ± 1.84; 6-OHDA, 3.33 ± 0.62; 6-OHDA and/or hASC, 42 ± 1.69; $p < 0.05$; Fig. 2D).

Based on these findings, we concluded that hASC transplantation rescued the dopaminergic neurons in the SN and functionally improved the level of dopamine transmission.

3.3. Ruptured and damaged mitochondria were decreased by hASC injection in the region of the SN in the PD mouse model

Many studies have reported structural and functional modifications of the mitochondria in various neurodegenerative diseases, including PD, Alzheimer's disease and amyotrophic lateral sclerosis (Lin and Beal, 2006). Therefore, we focused on the characteristics of the mitochondria in the PD mouse model with or without hASC transplantation. To investigate whether hASC are responsible for the recovery of damaged mitochondria in the region of the SN, we observed the level of structural degeneration of mitochondria using a TEM. Abnormal structural features, such as the ruptured membrane and collapsed cristae, were observed in the damaged mitochondria in the SN of the 6-OHDA-induced PD mice (Fig. 3A). The number of damaged mitochondria was significantly increased in the 6-OHDA-induced PD group compared with the control group (Fig. 3A and B). This morphological damage was decreased by the transplantation of hASC (Fig. 3A). The number of undamaged and damaged mitochondria was counted. Each area denoted marked with an asterisk in the 4 figures was enlarged and is shown on the right of Fig. 3A. The percent of undamaged (Fig. 3B top) or damaged (Fig. 3B bottom) mitochondria was calculated and is represented by the bar graphs. In the 6-OHDA and hASC group, the population of damaged mitochondria was significantly decreased (22.56%, $p < 0.001$), compared to the 6-OHDA group (Fig. 3B). (Undamaged mitochondria, saline, 91.66 ± 1.13; saline and/or hASC, 95.46 ± 0.71; 6-OHDA, 70.50 ± 3.18%; 6-OHDA and/or hASC, 93.06 ± 0.85%).

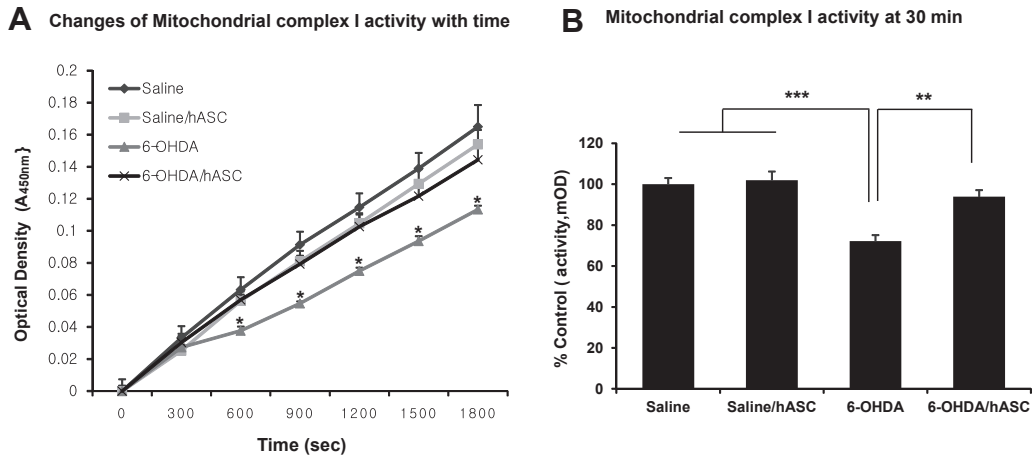

Fig. 4. Mitochondrial complex I activity was restored in hASC-transplanted Parkinson's disease (PD) mice. Mitochondrial complex I activity was measured using the brain tissue lysate of the substantia nigra. Decreased mitochondrial complex I activity by 6-OHDA was restored in the brain of the hASC-injected PD mouse model. (A) The optical density value was measured every minute for 30 minutes. (B) The enzyme activity (mOD/time) is represented as a percentage compared to the control. (Saline, 100 ± 3.05%; saline and/or hASC, 101.94 ± 4.24%; 6-OHDA, 72.21 ± 2.94%; 6-OHDA and/or hASC, 93.94 ± 3.20%) ***$p < 0.001$; **$p < 0.01$; *$p < 0.05$ by 1-way analysis of variance, Tukey's multiple comparisons test. Abbreviations: hASC, human adipose-derived stem cells; 6-OHDA, 6-hydroxydopamine.

3.4. Decreased mitochondrial complex I activity was restored in the SN of hASC-injected PD mouse model

To confirm the effect of hASC in the function of mitochondria, we performed a mitochondrial enzyme activity assay related to the mitochondrial respiratory chain. The SN region was isolated in 4 mouse brains per group and homogenized with PBS. Mitochondrial complex I was immunocaptured from tissue lysate within the wells of the microplate, and the activity was determined by the oxidation of nicotinamide adenine dinucleotide to NAD+ and the reduction of a dye that resulted in the increase in absorbance at 450 nm.

Mitochondrial complex I, a nicotinamide adenine dinucleotide–quinone oxidoreductase, is the first enzyme in the mitochondrial respiratory chain and has been highlighted as a factor in the etiology of PD (Marella et al., 2009). Decreased complex I activity ultimately leads to dopaminergic neuronal cell death, producing reactive oxygen species and a decreased energy supply (Abou-Sleiman et al., 2006; Marella et al., 2009). In our study, mitochondrial complex I activity was decreased by 6-OHDA, which is known to inhibit mitochondrial complex I. During the 30-minute reaction, the maximum optical density at 450 nm is shown in Fig. 4A. The activity of this enzyme was restored by the transplantation of hASC. PD group showed a significant decrease in mitochondrial complex I activity (27.78%, $p < 0.001$), and hASC injection restored the activity to control levels (21.72%, $p < 0.01$) (Fig. 4B); saline, 100 ± 3.05%; saline and/or hASC, 101.94 ± 4.24%; 6-OHDA, 72.21 ± 2.94%; 6-OHDA and/or hASC, 93.94 ± 3.20%.

4. Discussion

Chronic neurodegenerative diseases, including PD, Alzheimer's disease, and Huntington disease could be caused by aging, which are characterized by gradually progressive and selective neuronal loss. This pathological characteristic results in marked dysfunction of the neural system with a concomitant lack of the neurotransmitter. In particular, PD involves dopaminergic neuronal loss and the depletion of dopamine. Therefore, the goal of cell-based therapies for PD is the replacement of dopaminergic neurons in the SN or the protection of these neurons from further loss (Joyce et al., 2010). Recent studies have been showed that MSCs displayed neuroprotective effect through autophagy modulation (Park et al., 2014), and dopaminergic carotid body grafts could protect SN dopaminergic neuronal degeneration in an MPTP (1-methyl-4-phenyl-1,2,3,6-tetrahydropyridine)-induced PD mouse model (Munoz-Manchado et al., 2013).

The ideal cell sources for the treatment of neurodegenerative disease are easily obtained in abundant quantities, can differentiate into multiple cell lineages, and can have high-proliferation ability in vitro. The hASC used in this study can be separated easily from adipose tissue and have a multipotent ability to differentiate into neural cells (Zuk et al., 2002). Several studies recently reported that ASCs had multilineage differentiation potential and could differentiate into neuron-like cells in the neurogenic induction medium, displaying morphological changes and the expression of neuronal markers, such as β-tubulin III (Tuj-1) and glial fibrillary acidic protein (Wang et al., 2013a; Ying et al., 2012). In addition, because immune rejection, tumorigenesis or ethical problems may be resolved by the use of autologous cells, hASC may be applied for PD treatment as a potential source for cellular therapy.

In this study, the potential application of hASC for PD treatment was verified using the intravenous transplantation of hASC in the 6-OHDA-induced PD mouse model. Injected hASC improved motor performance in the PD mouse model. The intravenous implantation of hASC could be a more convenient approach for the recovery of damage than direct implantation into the brain. Therefore, this method can be a useful therapeutic strategy for PD and other neurodegenerative diseases.

6-OHDA-induced mouse model among several neurotoxin models was used for this study. This 6-OHDA model has a merit that displays the hallmarks of PD. Though this model shows the disease at end stage, it may be appropriate in the research of stem cell therapy replacing cells for neuronal loss which proceeds according to aging. Oxidative stress caused by 6-OHDA led to dopaminergic neuronal cell death and mitochondrial dysfunction. Many studies have reported that the structural and functional modifications of cytosolic mitochondria were related to various neurodegenerative diseases (Dexter et al., 1989; Moon et al., 2013; Shim et al., 2011; Sriram et al., 1997). For that reason, this study preferentially evaluated the effect of hASC on mitochondrial dysfunction.

Previous studies suggest that the effectiveness of hASC transplantation might be attributed to their immunomodulatory,

anti-inflammatory, and neurotrophic effects. In PD mice, the transplantation of hASC exerted beneficial pathological effects including the recovery of dopaminergic neurons and the restoration of cytosolic mitochondria.

PET imaging with raclopride, a dopamine D_2 receptor antagonist, showed an increased striatal dopamine level in hASC- transplanted PD mice. We confirmed the recovery of dopaminergic neurons in the SN by assessing the immunostained dopaminergic neurons with an anti-TH antibody. These results showed decreased dopaminergic neuronal cell death in hASC-injected PD mouse brains. The restored dopaminergic cell death could be explained by recovering the mitochondrial dysfunction. In the hASC-transplanted PD mouse brains, the undamaged mitochondrial population was increased. Interestingly, we also found an increased level of mitochondrial complex I activity, which provides molecular evidence for the recovery of mitochondrial function. Based on these results, treatment with hASC may be expected to alleviate the symptoms of the disease or slow the progression.

However, because there are many controversies about whether hASC differentiate into neurons or mesenchymal tissue supporting neurons, more research concerning the mechanisms involved in the neuronal differentiation will be necessary. Moreover, the specific marker for hASC isolation from the stromal vascular fraction should be developed for the preparation of hASC as therapeutic cell source for PD. If the therapeutic potential of hASC is verified through these further studies, it is expected to contribute to the breakthrough in the treatment of PD.

As the elderly population increases, the incidence of neurodegenerative diseases and socioeconomic cost to treat it are increasing. This study could suggest a potential possibility to develop one of the candidates for the treatment of neurodegenerative diseases including PD.

Disclosure statement

The authors have no conflicts of interest to disclose.

Acknowledgements

The authors are grateful to Dr. Hyun-Ho Lim for the critical reading of manuscript. This research was supported by KBRI Basic Research Program though Korea Brain Research Institute funded by the Ministry of Science, ICT and Future Planning (grant number 2231–415) and a grant of the Korea Health Technology R&D Project through the Korea Health Industry Development Institute (KHIDI), funded by the Ministry of Health and Welfare, South Korea (grant number: H I14C1135). The funders had no role in the study design, data collection and analysis, decision to publish, or preparation of the manuscript. Yoo-Hun Suh and Keun-A Chang supervised the project and designed the experiments. Hee Soon Choi and Hee Jin Kim carried out the experiments, analyzed data, and wrote the manuscript. Jin-Hwan Oh analyzed the PET imaging data. Hyeong-Geun Park and Jeong Chan Ra performed the isolation and culture of hASC. All authors performed data quantification, discussed the results, and commented on the manuscript.

Appendix A. Supplementary data

Supplementary data associated with this article can be found, in the online version at http://dx.doi.org/10.1016/j.neurobiolaging.2015.06.022.

References

Abou-Sleiman, P.M., Muqit, M.M., Wood, N.W., 2006. Expanding insights of mitochondrial dysfunction in Parkinson's disease. Nat. Rev. Neurosci. 7, 207–219.
Amariglio, N., Hirshberg, A., Scheithauer, B.W., Cohen, Y., Loewenthal, R., Trakhtenbrot, L., Paz, N., Koren-Michowitz, M., Waldman, D., Leider-Trejo, L., Toren, A., Constantini, S., Rechavi, G., 2009. Donor-derived brain tumor following neural stem cell transplantation in an ataxia telangiectasia patient. PLoS Med. 6, e1000029.
Bennett, D.A., Beckett, L.A., Murray, A.M., Shannon, K.M., Goetz, C.G., Pilgrim, D.M., Evans, D.A., 1996. Prevalence of parkinsonian signs and associated mortality in a community population of older people. N. Engl. J. Med. 334, 71–76.
Ben-Shachar, D., Zuk, R., Glinka, Y., 1995. Dopamine neurotoxicity: inhibition of mitochondrial respiration. J. Neurochem. 64, 718–723.
Bjorklund, L.M., Sanchez-Pernaute, R., Chung, S., Andersson, T., Chen, I.Y., McNaught, K.S., Brownell, A.L., Jenkins, B.G., Wahlestedt, C., Kim, K.S., Isacson, O., 2002. Embryonic stem cells develop into functional dopaminergic neurons after transplantation in a Parkinson rat model. Proc. Natl. Acad. Sci. U. S. A. 99, 2344–2349.
Brederlau, A., Correia, A.S., Anisimov, S.V., Elmi, M., Paul, G., Roybon, L., Morizane, A., Bergquist, F., Riebe, I., Nannmark, U., Carta, M., Hanse, E., Takahashi, J., Sasai, Y., Funa, K., Brundin, P., Eriksson, P.S., Li, J.Y., 2006. Transplantation of human embryonic stem cell-derived cells to a rat model of Parkinson's disease: effect of in vitro differentiation on graft survival and teratoma formation. Stem Cells 24, 1433–1440.
Chang, K.A., Kim, H.J., Joo, Y., Ha, S., Suh, Y.H., 2014. The therapeutic effects of human adipose-derived stem cells in Alzheimer's disease mouse models. Neurodegener Dis. 13, 99–102.
Collier, T.J., Kanaan, N.M., Kordower, J.H., 2011. Ageing as a primary risk factor for Parkinson's disease: evidence from studies of non-human primates. Nat. Rev. Neurosci. 12, 359–366.
Dexter, D.T., Wells, F.R., Lees, A.J., Agid, F., Agid, Y., Jenner, P., Marsden, C.D., 1989. Increased nigral iron content and alterations in other metal ions occurring in brain in Parkinson's disease. J. Neurochem. 52, 1830–1836.
Dragicevic, E., Poetschke, C., Duda, J., Schlaudraff, F., Lammel, S., Schiemann, J., Fauler, M., Hetzel, A., Watanabe, M., Lujan, R., Malenka, R.C., Striessnig, J., Liss, B., 2014. Cav1.3 channels control D2-autoreceptor responses via NCS-1 in substantia nigra dopamine neurons. Brain 137, 2287–2302.
Duinsbergen, D., Salvatori, D., Eriksson, M., Mikkers, H., 2009. Tumors originating from induced pluripotent stem cells and methods for their prevention. Ann. N. Y. Acad. Sci. 1176, 197–204.
Frazier, A.E., Kiu, C., Stojanovski, D., Hoogenraad, N.J., Ryan, M.T., 2006. Mitochondrial morphology and distribution in mammalian cells. Biol. Chem. 387, 1551–1558.
Gasser, T., 2009. Mendelian forms of Parkinson's disease. Biochim. Biophys. Acta 1792, 587–596.
Gazewood, J.D., Richards, D.R., Clebak, K., 2013. Parkinson disease: an update. Am. Fam. Physician 87, 267–273.
Glavaski-Joksimovic, A., Bohn, M.C., 2013. Mesenchymal stem cells and neuroregeneration in Parkinson's disease. Exp. Neurol. 247, 25–38.
Glinka, Y., Tipton, K.F., Youdim, M.B., 1996. Nature of inhibition of mitochondrial respiratory complex I by 6-Hydroxydopamine. J. Neurochem. 66, 2004–2010.
Glinka, Y.Y., Youdim, M.B., 1995. Inhibition of mitochondrial complexes I and IV by 6-hydroxydopamine. Eur. J. Pharmacol. 292, 329–332.
Joyce, N., Annett, G., Wirthlin, L., Olson, S., Bauer, G., Nolta, J.A., 2010. Mesenchymal stem cells for the treatment of neurodegenerative disease. Regen. Med. 5, 933–946.
Kim, H.J., Chang, K.A., Ha, T.Y., Kim, J., Ha, S., Shin, K.Y., Moon, C., Nacken, W., Kim, H.S., Suh, Y.H., 2014. S100A9 knockout decreases the memory impairment and neuropathology in crossbreed mice of Tg2576 and S100A9 knockout mice model. PLoS One 9, e88924.
Kim, S., Chang, K.A., Kim, J., Park, H.G., Ra, J.C., Kim, H.S., Suh, Y.H., 2012. The preventive and therapeutic effects of intravenous human adipose-derived stem cells in Alzheimer's disease mice. PLoS One 7, e45757.
Lin, M.T., Beal, M.F., 2006. Mitochondrial dysfunction and oxidative stress in neurodegenerative diseases. Nature 443, 787–795.
Marella, M., Seo, B.B., Yagi, T., Matsuno-Yagi, A., 2009. Parkinson's disease and mitochondrial complex I: a perspective on the Ndi1 therapy. J. Bioenerg. Biomembr 41, 493–497.
Mizuno, Y., Ohta, S., Tanaka, M., Takamiya, S., Suzuki, K., Sato, T., Oya, H., Ozawa, T., Kagawa, Y., 1989. Deficiencies in complex I subunits of the respiratory chain in Parkinson's disease. Biochem. Biophys Res. Commun. 163, 1450–1455.
Moon, H.E., Yoon, S.H., Hur, Y.S., Park, H.W., Ha, J.Y., Kim, K.H., Shim, J.H., Yoo, S.H., Son, J.H., Paek, S.L., Kim, I.K., Hwang, J.H., Kim, D.G., Kim, H.J., Jeon, B.S., Park, S.S., Paek, S.H., 2013. Mitochondrial dysfunction of immortalized human adipose tissue-derived mesenchymal stromal cells from patients with Parkinson's disease. Exp. Neurobiol. 22, 283–300.
Morens, D.M., Davis, J.W., Grandinetti, A., Ross, G.W., Popper, J.S., White, L.R., 1996. Epidemiologic observations on Parkinson's disease: incidence and mortality in a prospective study of middle-aged men. Neurology 46, 1044–1050.
Munoz-Manchado, A.B., Villadiego, J., Suarez-Luna, N., Bermejo-Navas, A., Garrido-Gil, P., Labandeira-Garcia, J.L., Echevarria, M., Lopez-Barneo, J., Toledo-Aral, J.J.,

2013. Neuroprotective and reparative effects of carotid body grafts in a chronic MPTP model of Parkinson's disease. Neurobiol. Aging 34, 902–915.
Murrell, W., Wetzig, A., Donnellan, M., Feron, F., Burne, T., Meedeniya, A., Kesby, J., Bianco, J., Perry, C., Silburn, P., Mackay-Sim, A., 2008. Olfactory mucosa is a potential source for autologous stem cell therapy for Parkinson's disease. Stem Cells 26, 2183–2192.
Oh, J.Y., Lee, H.J., Khwarg, S.I., Wee, W.R., 2010. Corneal cell viability and structure after transcorneal freezing-thawing in the human cornea. Clin. Ophthalmol. 4, 477–480.
Olanow, C.W., Schapira, A.H., 2013. Therapeutic prospects for Parkinson disease. Ann. Neurol. 74, 337–347.
Pankratz, N., Foroud, T., 2007. Genetics of Parkinson disease. Genet. Med. 9, 801–811.
Park, H.J., Shin, J.Y., Kim, H.N., Oh, S.H., Lee, P.H., 2014. Neuroprotective effects of mesenchymal stem cells through autophagy modulation in a parkinsonian model. Neurobiol. Aging 35, 1920–1928.
Shim, J.H., Yoon, S.H., Kim, K.H., Han, J.Y., Ha, J.Y., Hyun, D.H., Paek, S.H., Kang, U.J., Zhuang, X., Son, J.H., 2011. The antioxidant Trolox helps recovery from the familial Parkinson's disease-specific mitochondrial deficits caused by PINK1- and DJ-1-deficiency in dopaminergic neuronal cells. Mitochondrion 11, 707–715.
Shirpoor, A., Salami, S., Khadem-Ansari, M.H., Ilkhanizadeh, B., Pakdel, F.G., Khademvatani, K., 2009. Cardioprotective effect of vitamin E: rescues of diabetes-induced cardiac malfunction, oxidative stress, and apoptosis in rat. J. Diabetes Complications 23, 310–316.
Soto-Otero, R., Mendez-Alvarez, E., Sanchez-Iglesias, S., Zubkov, F.I., Voskressensky, L.G., Varlamov, A.V., de Candia, M., Altomare, C., 2008. Inhibition of 6-hydroxydopamine-induced oxidative damage by 4,5-dihydro-3H-2-benzazepine N-oxides. Biochem. Pharmacol. 75, 1526–1537.
Spillantini, M.G., Schmidt, M.L., Lee, V.M., Trojanowski, J.Q., Jakes, R., Goedert, M., 1997. Alpha-synuclein in Lewy bodies. Nature 388, 839–840.
Sriram, K., Pai, K.S., Boyd, M.R., Ravindranath, V., 1997. Evidence for generation of oxidative stress in brain by MPTP: in vitro and in vivo studies in mice. Brain Res. 749, 44–52.
Stott, S.R., Barker, R.A., 2014. Time course of dopamine neuron loss and glial response in the 6-OHDA striatal mouse model of Parkinson's disease. Eur. J. Neurosci. 39, 1042–1056.
Tanner, C.M., Goldman, S.M., 1996. Epidemiology of Parkinson's disease. Neurol. Clin. 14, 317–335.
Tomita, K., Madura, T., Sakai, Y., Yano, K., Terenghi, G., Hosokawa, K., 2013. Glial differentiation of human adipose-derived stem cells: implications for cell-based transplantation therapy. Neuroscience 236, 55–65.
Traktuev, D.O., Merfeld-Clauss, S., Li, J., Kolonin, M., Arap, W., Pasqualini, R., Johnstone, B.H., March, K.L., 2008. A population of multipotent CD34-positive adipose stromal cells share pericyte and mesenchymal surface markers, reside in a periendothelial location, and stabilize endothelial networks. Circ. Res. 102, 77–85.
Venkataramana, N.K., Kumar, S.K., Balaraju, S., Radhakrishnan, R.C., Bansal, A., Dixit, A., Rao, D.K., Das, M., Jan, M., Gupta, P.K., Totey, S.M., 2010. Open-labeled study of unilateral autologous bone-marrow-derived mesenchymal stem cell transplantation in Parkinson's disease. Transl. Res. 155, 62–70.
Wang, Q., Zhou, L., Guo, Y., Liu, G., Cheng, J., Yu, H., 2013a. Differentiation of human adipose-derived stem cells into neuron-like cells by Radix Angelicae Sinensis. Neural Regen. Res. 8, 3353–3358.
Wang, Y.H., Yu, H.T., Pu, X.P., Du, G.H., 2013b. Baicalein prevents 6-hydroxydopamine-induced mitochondrial dysfunction in SH-SY5Y cells via inhibition of mitochondrial oxidation and up-regulation of DJ-1 protein expression. Molecules 18, 14726–14738.
Xu, W., Liu, W., Shao, X., Jiang, G., Li, X., 2012. Effect of trichlorfon on hepatic lipid accumulation in crucian carp Carassius auratus gibelio. J. Aquat. Anim. Health 24, 185–194.
Ying, C., Hu, W., Cheng, B., Zheng, X., Li, S., 2012. Neural differentiation of rat adipose-derived stem cells in vitro. Cell Mol. Neurobiol. 32, 1255–1263.
Zuk, P.A., Zhu, M., Ashjian, P., De Ugarte, D.A., Huang, J.I., Mizuno, H., Alfonso, Z.C., Fraser, J.K., Benhaim, P., Hedrick, M.H., 2002. Human adipose tissue is a source of multipotent stem cells. Mol. Biol. Cel. 13, 4279–4295.